Int. J. Heat Mass Transfer. Vol. 35, No. 11, pp. 3069–3075, 1992
Printed in Great Britain

0017–9310/92 \$5.00+0.00
Pergamon Press Ltd

Heat transfer to generalized non-Newtonian Couette flow in annuli with moving outer cylinder

S. H. LIN

Department of Chemical Engineering, Yuan Ze Institute of Technology, Neili, Taoyuan 320, Taiwan, Republic of China

(*Received* 20 *October* 1991)

Abstract—Heat transfer to generalized Couette flow of a power-law non-Newtonian fluid in a concentric annulus with moving outer cylinder is investigated. Velocity distribution equations in integral form are developed for the generalized flow in which the maximum velocity may occur between the two cylinders or at the moving outer cylinder, depending on the imposed pressure gradient. The heat transfer model, which includes the viscous dissipation, is numerically simulated for the boundary conditions of constant cylinder temperature. The present numerical solutions agree very well with the previous semi-analytic ones for a special case. The effects of several dimensionless parameters such as the reciprocal of pressure gradient, pseudoplastic index and viscous dissipation parameter, on the heat transfer characteristics are explored.

1. INTRODUCTION

STUDIES of heat transfer characteristics of non-Newtonian fluids in conduits have been of great practical significance primarily because of its potential applications in many areas of applied sciences, such as polymer and food processings [1, 2]. In particular, polymer coatings on plates, wires or tubes for corrosion resistance or protection have been gaining wide industrial acceptance in recent years [3]. Investigations of the heat transfer characteristics of non-Newtonian fluids can lead to considerable understanding of the fundamental aspects of this process.

Hong and Mathews [4] treated the heat transfer problem of ordinary non-Newtonian flow in concentric annuli. Lin, the present author, considered previously the heat transfer problems of generalized Couette non-Newtonian flow between parallel plates with one moving plate [5] and in concentric annuli with moving inner cylinder [6]. One problem of comparable practical significance has not received any attention thus far. This is the heat transfer to generalized non-Newtonian flow in concentric annuli with moving outer cylinder. This problem may simulate the polymer coating inside a tube. In fact, metal tubes with appropriate polymer inner linings have been widely used in chemical process industries for transporting corrosive fluids for years [3]. Although this problem shows some similarities in appearance to that considered by Lin and Hsieh [6], they do have a marked difference in the flow patterns and thus the heat transfer characteristics. The present investigation is to consider the heat transfer problem to generalized power-law non-Newtonian flow in annuli with moving outer cylinder.

2. VELOCITY DISTRIBUTION OF FLOW

The velocity distribution of the present problem has not been available in the open literature. It has to be determined before the heat transfer investigations can be undertaken, hence the equations of velocity distribution need to be developed first.

Considering a steady, one-dimensional flow, the momentum balance equation is represented by

$$\frac{1}{r}\frac{\mathrm{d}}{\mathrm{d}r}(\tau r) = -\frac{\mathrm{d}P}{\mathrm{d}x}. \tag{1}$$

Assuming a constant axial pressure gradient, the above equation can be integrated to yield

$$\tau = \left(-\frac{\mathrm{d}P}{\mathrm{d}x}\right)r + \frac{c}{r} \tag{2}$$

c being the integration constant.

The velocity distribution for the generalized non-Newtonian flow in annuli can be divided into two types. The first type is that when the imposed pressure gradient is not sufficiently strong, the maximum velocity occurs at the moving outer cylinder. The second one is that the pressure gradient is strong enough to create a maximum velocity between the two cylinders. These two cases need to be treated separately.

If the maximum velocity occurs at the moving outer cylinder, the velocity gradient is positive over the flow region. The shear stress for a power-law fluid can be represented by

$$\tau = -m\left(\frac{\mathrm{d}v}{\mathrm{d}r}\right)^n. \tag{3}$$

NOMENCLATURE

A	dimensionless integration constant, $(-c/mr_0\alpha)^{1/2}$
c	integration constant
C_p	specific heat
k	dimensionless radius of inner cylinder
k_1	thermal conductivity of fluid
m	consistency index
n	pseudoplastic index
Nu	Nusselt number, $2r_0h/k_1$
p	pressure
r	radial coordinate
r_0	radius of outer cylinder
R	dimensionless radial coordinate, r/r_0
T	temperature
T_0	inlet fluid temperature
T_1	wall temperature of inner cylinder
T_2	water temperature of outer cylinder
$\langle T\rangle$	bulk temperature
U	dimensionless velocity, v/V
U_1, U_2	dimensionless velocities, v_1/V and v_2/V
v	local velocity
v_1, v_2	local velocities in regions 1 and 2
V	constant velocity of moving outer cylinder
z	axial coordinate
Z	dimensionless axial coordinate, $zk_1/\rho C_p V r_0^2$.

Greek symbols

α	pressure gradient parameter, $(-r_0/2m)(dp/dz)$
β	reciprocal of the dimensionless pressure gradient parameter, $V/r_0\alpha^{1/n}$
γ	dimensionless wall temperature of the outer cylinder, $(T_2-T_1)/(T_0-T_1)$
θ	dimensionless temperature, $(T-T_1)/(T_0-T_1)$
$\langle\theta\rangle$	dimensionless bulk temperature, $(\langle T\rangle-T_1)/(T_0-T_1)$
ρ	density of fluid
σ	dimensionless parameter, $(\alpha^{1/n}r_0/V)^{n+1}(mV^{n+1})/[r_0^{n-1}k_1(T_0-T_1)]$
τ	shear stress.

Combining equations (2) and (3) and introducing appropriate dimensionless variables yields

$$\frac{dv}{dr}=\alpha^{1/n}\left(\frac{A^2}{R}-R\right)^{1/n}. \tag{4}$$

Using the boundary conditions $v=0$ at $r=kr_0$, equation (4) can be integrated

$$U=\frac{1}{\beta}\int_k^R\left(\frac{A^2}{R}-R\right)^{1/n}dR. \tag{5}$$

At the moving outer cylinder, $U=1$ and this condition is employed to determine A, hence it is obtained from equation (5)

$$\int_k^1\left(\frac{A^2}{R}-R\right)^{1/n}dR=\beta. \tag{6}$$

The method of false position [7] is used to determine the value of A in terms of n, k and β.

For the second type of fluid flow with strong imposed pressure gradient, the velocity distribution can be divided into two regions because of the appearance of a maximum velocity between the two cylinders. The first region is between the point of maximum velocity and the moving outer cylinder. Due to the negative velocity gradient in this region, the shear stress equation becomes

$$\tau=m\left(-\frac{dv_1}{dr}\right)^n. \tag{7}$$

Combining equations (2) and (7) gives

$$\frac{dv_1}{dr}=-\alpha^{1/n}\left(R-\frac{A^2}{R}\right)^{1/n}. \tag{8}$$

Using the boundary condition $v_1=V$ at $R=1$, equation (8) can be integrated to yield

$$U_1=1+\frac{1}{\beta}\int_R^1\left(R-\frac{A^2}{R}\right)^{1/n}dR \quad \text{for} \quad A\leqslant R\leqslant 1. \tag{9}$$

Note that A is the location where the maximum velocity occurs. This can be easily seen from equation (8) because the velocity gradient disappears at the point of maximum velocity or at $R=A$.

In the second region between the point of maximum velocity and the inner cylinder, the velocity gradient is positive, just like that of the first type of flow, hence equation (5) still is applicable and can be rewritten as

$$U_2=\frac{1}{\beta}\int_k^R\left(\frac{A^2}{R}-R\right)^{1/n}dR \quad \text{for} \quad k\leqslant R\leqslant A. \tag{10}$$

To determine the numerical values of A for the present case, the boundary condition $U_1=U_2$ at $R=A$ can be used, hence it is obtained from equations (9) and (10)

$$\int_k^A\left(\frac{A^2}{R}-R\right)^{1/n}dR-\int_A^1\left(R-\frac{A^2}{R}\right)^{1/n}dR=\beta. \tag{11}$$

Again the numerical values of A were also computed

Table 1. Numerical values of A in terms of n and β with $k = 0.4$

β	n = 0.2	0.4	0.6	0.8	1.0
0.005	0.67514	0.66984	0.67414	0.67800	0.68105
0.010	0.69264	0.67764	0.67956	0.68248	0.68504
0.015	0.70607	0.68512	0.68488	0.68692	0.68901
0.020	0.71689	0.69228	0.69011	0.69131	0.69296
0.025	0.72589	0.69913	0.69526	0.69567	0.69689
0.04	0.74659	0.71812	0.71023	0.70851	0.70854
0.06	0.76590	0.74031	0.72912	0.72517	0.72378
0.08	0.78047	0.75960	0.74689	0.74127	0.73870
0.10	0.79227	0.77663	0.76363	0.75685	0.75333
0.12	0.80216	0.79187	0.77945	0.77197	0.76768
0.14	0.81070	0.80566	0.79444	0.78662	0.78177
0.16	0.81822	0.81826	0.80866	0.80085	0.79561
0.18	0.82496	0.82986	0.82220	0.81468	0.80921
0.2	0.83106	0.84061	0.83511	0.82813	0.82258
0.3	0.85528	0.88521	0.89191	0.89033	0.88644
0.4	0.87320	0.91984	0.93904	0.94546	0.94600
0.5	0.88753	0.94838	0.97937	0.99486	1.00202
0.6	0.89952	0.97280	1.01463	1.03944	1.05508
0.8	0.91897	1.01339	1.07480	1.11859	1.15389
1.0	0.93452	1.04669	1.12577	1.18852	1.24488
2.0	0.98546	1.16126	1.31258	1.46279	1.62514
5.0	1.05939	1.34282	1.64135	1.99517	2.43211
10.0	1.12068	1.50767	1.96822	2.56997	2.37223
∞	∞	∞	∞	∞	∞

Table 2. Numerical values of A in terms of n and β with $k = 0.8$

β	n = 0.2	0.4	0.6	0.8	1.0
0.001	1.01862	0.92241	0.90468	0.90157	0.90063
0.002	1.04314	0.94234	0.91175	0.90527	0.90312
0.003	1.05865	0.95787	0.91864	0.90894	0.90559
0.004	1.07020	0.97044	0.92533	0.91259	0.90807
0.005	1.07950	0.98101	0.93181	0.91621	0.91053
0.006	1.08731	0.99015	0.93806	0.91981	0.91299
0.007	1.09407	0.99824	0.94409	0.92338	0.91544
0.008	1.10005	1.00552	0.94989	0.92692	0.91788
0.009	1.10542	1.01213	0.95548	0.93043	0.92032
0.010	1.11030	1.01824	0.96085	0.93391	0.92275
0.012	1.11891	1.02921	0.97095	0.94078	0.92760
0.014	1.12637	1.03892	0.98040	0.94753	0.93241
0.016	1.13296	1.04767	0.98913	0.95414	0.93721
0.018	1.13887	1.05567	0.99725	0.96063	0.94198
0.020	1.14425	1.06306	1.00484	0.96699	0.94672
0.025	1.15590	1.07945	1.02196	0.98227	0.95848
0.030	1.16569	1.09365	1.03723	0.99666	0.97010
0.035	1.17417	1.10626	1.05114	1.01014	0.98158
0.040	1.18166	1.11765	1.06400	1.02287	0.99293
0.045	1.18839	1.12808	1.07603	1.03504	1.00415
0.050	1.19450	1.13772	1.08737	1.04675	1.01525
0.075	1.21887	1.17775	1.13656	1.10013	1.06900
0.1	1.23701	1.20918	1.17753	1.14752	1.12018
0.2	1.28370	1.29633	1.30123	1.30355	1.30497
0.3	1.31330	1.35639	1.39305	1.42931	1.46666
0.4	1.33525	1.40317	1.46839	1.53746	1.61221
0.5	1.35287	1.44206	1.53324	1.63363	1.74568
0.75	1.38628	1.51902	1.66689	1.83939	2.04150
1.0	1.41110	1.57889	1.77524	2.01268	2.29958
2.0	1.47496	1.74283	2.08910	2.54101	3.12562
5.0	1.56855	2.00802	2.64119	3.54525	4.81807
10.0	1.64743	2.25103	3.18751	4.61372	6.75432
∞	∞	∞	∞	∞	∞

iteratively. Some typical values are given in Tables 1 and 2 in terms of n, k and β. The values above the broken lines are for the second case with a maximum velocity between the two cylinders while those below are for the first case with a maximum velocity at the moving outer cylinder. Figure 1 shows the velocity distribution for different values of β.

An analytical expression for determining A can be obtained from equations (6) and (11) as a special case. When $n = 1$, both equations reduce to

$$A = \left([\beta + \tfrac{1}{2}(1-k^2)]\frac{1}{\ln(k)}\right)^{1/2}. \qquad (12)$$

For this particular case, the numerical values of A obtained by the iterative method agree very well with those obtained from equation (12) with the difference being less than 10^{-4}.

3. THE HEAT TRANSFER MODEL

For a steady state non-Newtonian flow with constant physical properties, the heat transfer equation with viscous dissipation can be represented by

$$\rho C_p v \frac{\partial T}{\partial z} = k_1 \left(\frac{\partial^2 T}{\partial r^2} + \frac{1}{r}\frac{\partial T}{\partial r}\right) - \tau \left(\frac{\mathrm{d}v}{\mathrm{d}r}\right). \qquad (13)$$

In dimensionless form, equation (13) can be rewritten as

$$U(R)\frac{\partial \theta}{\partial Z} = \frac{\partial^2 \theta}{\partial R^2} + \frac{1}{R}\frac{\partial \theta}{\partial R} + \sigma f(R) \qquad (14)$$

where $U(R)$ is the velocity distribution as given by equation (5) for the first case and by equations (9) and (10) for the second case. The viscous dissipation function $f(R)$ is represented by

$$f(R) = \left(\frac{A^2}{R} - R\right)^{(n+1)/n} \qquad (15)$$

for the first case with a maximum velocity at the outer moving cylinder and by

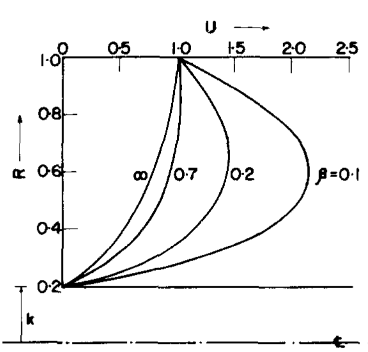

FIG. 1. Velocity distribution for different values of β with $k = 0.2$ and $n = 0.6$.

$$f(R) = \left(R - \frac{A^2}{R}\right)^{(n+1)/n} \qquad A \leqslant R \leqslant 1 \qquad (16)$$

$$= \left(\frac{A^2}{R} - R\right)^{(n+1)/n} \qquad k \leqslant R \leqslant A \qquad (17)$$

for the second case with a maximum velocity between two cylinders.

The inlet and boundary conditions in dimensionless form can be rewritten as

$$Z = 0; \quad \theta = 1 \qquad (18)$$

$$R = k; \quad \theta = 0 \qquad (19)$$

$$R = 1; \quad \theta = \gamma. \qquad (20)$$

The Nusselt number for this problem becomes

$$Nu_i = \frac{2}{\langle\theta\rangle}\left(\left.\frac{\partial\theta}{\partial R}\right|_{R=k}\right) \qquad (21)$$

for the inner cylinder and

$$Nu_o = \frac{2}{\langle\theta\rangle - \gamma}\left(\left.\frac{\partial\theta}{\partial R}\right|_{R=1}\right) \qquad (22)$$

for the outer cylinder. The bulk temperature $\langle\theta\rangle$ is defined as

$$\langle\theta\rangle = \frac{\int_k^1 \theta U(R) R \, \mathrm{d}R}{\int_k^1 U(R) R \, \mathrm{d}R}. \qquad (23)$$

Equation (14), along with the boundary conditions, equations (18)–(20), was numerically tackled by the implicit Crank–Nicolson finite difference method [7]. This method is computationally stable and very accurate. The dimensionless temperatures were generated first and then the bulk temperature and the Nusselt numbers were computed from equations (23), (21) and (22), respectively.

4. DISCUSSION OF RESULTS

To ascertain the accuracy of the numerical solutions obtained by the finite difference method employed in this study, several runs were made for heat transfer to non-Newtonian fluid in laminar flow through concentric annuli with stationary cylinders as a special case so that comparison can be made with the previous results. Figure 2 shows the present solutions and those of Hong and Mathews [4] for the outer Nusselt numbers. It is apparent that these two solutions are essentially identical. Other typical results for the present heat transfer problem are shown in the following figures.

Figure 3 displays the effect of the reciprocal of the dimensionless pressure gradient parameter β on the dimensionless bulk temperature. It is noted that near the channel entrance of $Z \leqslant 0.04$, the bulk temperature increases with decreasing β and beyond that

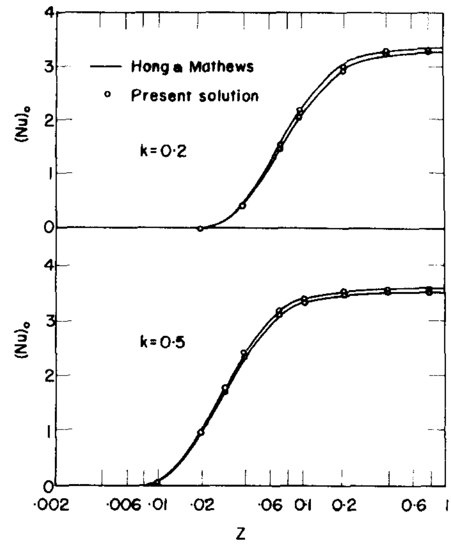

FIG. 2. Comparison of the outer Nusselt number obtained in this study with those of Hong and Mathews [4].

the situation is reversed. This phenomenon is significantly different from that with moving inner cylinder. The effect of β is in fact twofold. Small β implies a fast fluid flow which will result in a shorter fluid residence time inside the channel. A short flow residence time in turn means less heat loss and hence a higher bulk temperature will be expected. In the meantime, fast fluid flow also tends to increase the heat transfer rate. These two effects are opposite to each other. For the previous case with moving inner cylinder [6], the former effect outweighs the latter. For the present case, the former effect still dominates for $Z \leqslant 0.04$. For $Z > 0.04$, heat loss due to fast fluid flow tends, however, to outweigh the latter effect and

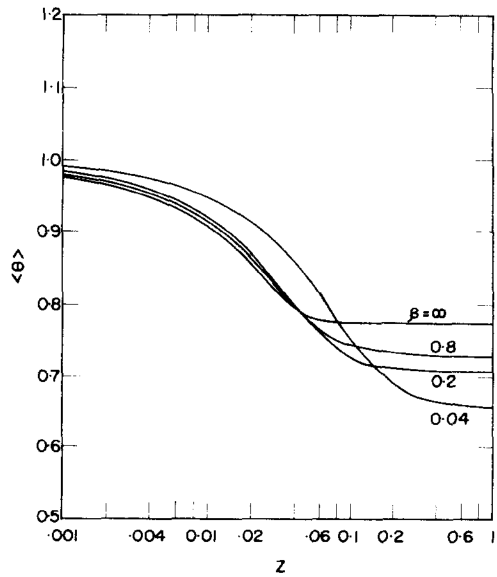

FIG. 3. Effect of the reciprocal of dimensionless pressure gradient on the dimensionless bulk temperature with $k = 0.4$, $n = 0.8$, $\sigma = 0$ and $\gamma = 1$.

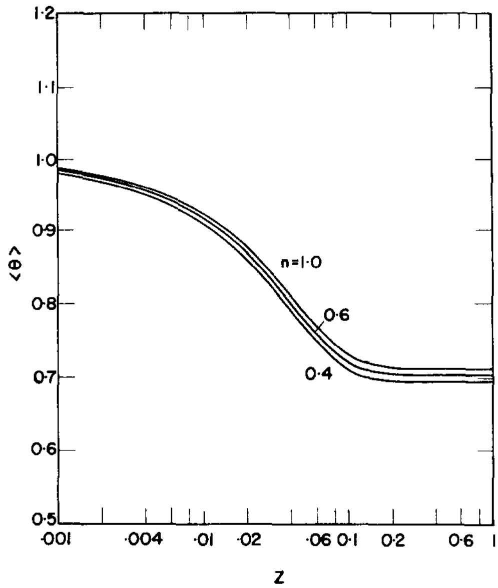

FIG. 4. Effect of the pseudoplastic index on the dimensionless bulk temperature with $k = 0.4$, $\beta = 0.2$, $\sigma = 0$ and $\gamma = 1$.

thus causes a lowering in the bulk fluid temperature at the thermally fully developed region as β decreases.

Figure 4 demonstrates the effect of the pseudoplastic index on the dimensionless bulk temperature. The general pattern of the bulk temperature profiles does not show much difference from that of the previous case [6] except that the effect of n seems to be more pronounced for the present case.

Viscous dissipation tends to increase the dimensionless bulk temperature because of irreversible conversion of mechanical energy to thermal energy. This holds true for the present case as well as the previous one. Figure 5 clearly displays very similar characteristic profiles of the dimensionless bulk temperature as those of the previous one [6].

The effect of the ratio of inner to outer radii on the dimensionless bulk temperature profiles is shown in Fig. 6. The bulk temperature decreases steadily with increasing Z until the temperature profiles are fully developed. The bulk temperature generally decreases with increasing k as anticipated except that the fully developed bulk temperature for $k = 0.8$ is only slightly higher than that for $k = 0.6$. The reason for this is not exactly known. It may be due to the fact that at $\beta = 0.04$ and $n = 0.8$ chosen for this illustration, the maximum velocity occurs between two cylinders for $k \leqslant 0.6$ while that with $k = 0.8$ occurs at the moving outer cylinder. Such a transition of maximum velocity from one type to the other could have a marked influence on the heat transfer rate and the bulk temperature profile.

Figure 7 shows the effect of the reciprocal of dimensionless pressure gradient parameter β on the Nusselt numbers. For this particular case with $k = 0.4$ and $n = 0.8$, the maximum velocity occurs at the moving outer cylinder when $\beta = 0.8$ but it takes place between the two cylinders when $\beta \leqslant 0.2$. Hence the velocity gradient at the inner cylinder wall is expected to increase with decreasing β. This contributes to an increase in the inner Nusselt number with decreasing β. At the outer cylinder wall, the situation is reversed. The velocity gradient at the cylinder wall decreases with decreasing β and so does the outer Nusselt number. The pseudoplastic index n seems to produce quite similar effects on the Nusselt number as displayed in Fig. 8. The only difference is that the effect of n on both Nu_i and Nu_o is less pronounced than that of β. It is also noted that in this figure that the effect of n seems to be diminishing as n approaches 1.

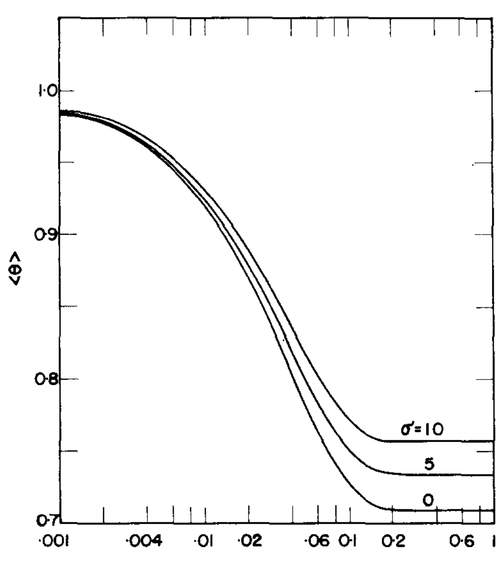

FIG. 5. Effect of viscous dissipation parameter on the dimensionless bulk temperature with $k = 0.4$, $n = 0.8$, $\beta = 0.2$ and $\gamma = 1$.

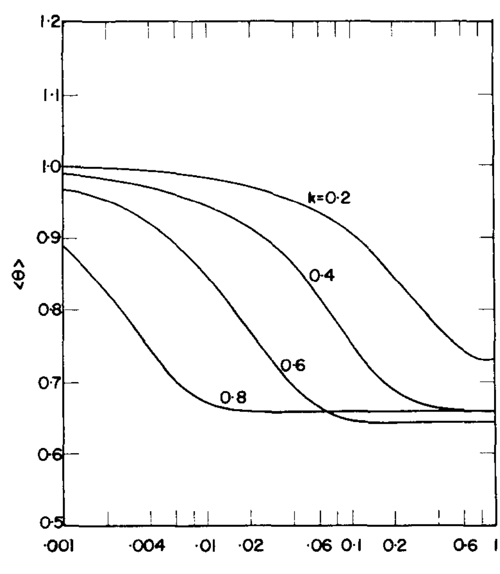

FIG. 6. Effect of the inner–outer radius ratio on the dimensionless bulk temperature with $k = 0.8$, $\beta = 0.04$, $\sigma = 0$ and $\gamma = 1$.

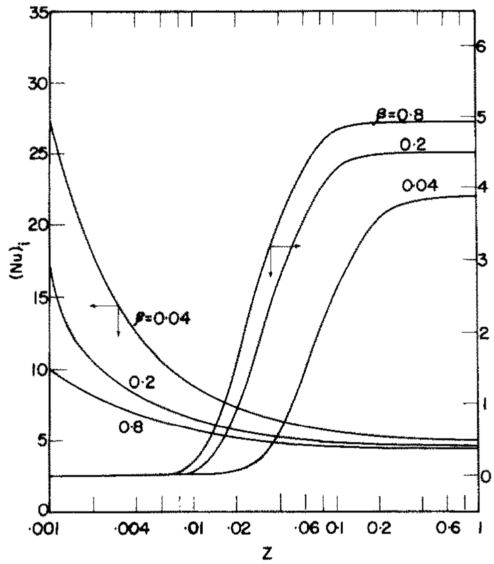

FIG. 7. Effect of the reciprocal of dimensionless pressure gradient on the Nusselt number with $k = 0.4$, $n = 0.8$, $\sigma = 0$ and $\gamma = 1$.

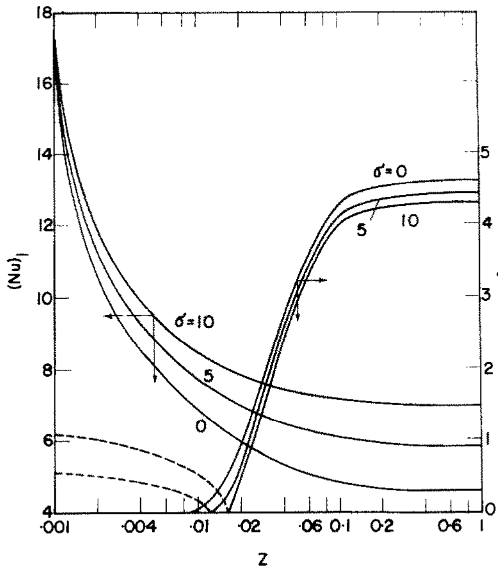

FIG. 9. Effect of viscous dissipation parameter on the Nusselt number with $k = 0.4$, $n = 0.8$, $\beta = 0.2$ and $\gamma = 1$.

Figure 9 examines the effect of viscous dissipation on the inner and outer Nusselt numbers. It is noted that viscous dissipation enhances the inner Nusselt number but suppresses the outer one. With viscous dissipation, the fluid temperature is generally maintained at a higher level than that without. This causes an increase in the temperature gradient at the inner cylinder and a decrease at the outer cylinder. With increasing viscous dissipation the inner Nusselt number is, therefore, proportionately increased while the outer one is decreased. The negative outer Nusselt number near the channel entrance for the case with viscous dissipation is due to the fact that the viscous dissipation rapidly boosts the local fluid temperature above its entrance level within a short distance from the entrance and thus causes a negative temperature gradient. This negative temperature gradient disappears further downstream because the heat loss through the cylinder walls is more than enough to compensate for the heat generation.

Figure 10 indicates that while the inner Nusselt number decreases with increasing k, the outer Nusselt number increases. This phenomenon is very similar to the effects of β and n. This is mainly due to the fact that as k decreases, the velocity gradient at the inner cylinder wall increases whereas that at the outer cylinder wall decreases.

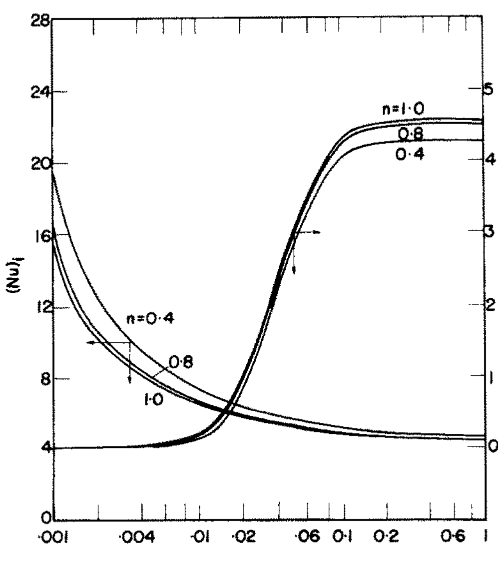

FIG. 8. Effect of the pseudoplastic index on the Nusselt number with $k = 0.4$, $\beta = 0.2$, $\sigma = 0$ and $\gamma = 1$.

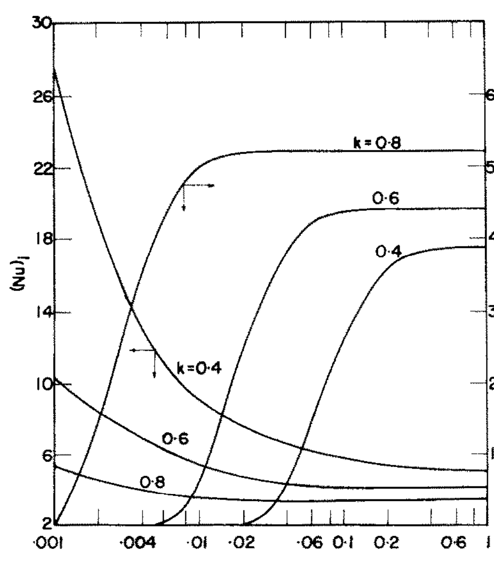

FIG. 10. Effect of the inner–outer radius ratio on the Nusselt number with $n = 0.8$, $\beta = 0.04$, $\sigma = 0$ and $\gamma = 1$.

5. CONCLUSIONS

An analytical procedure is presented in this paper for studying the heat transfer characteristics of a power-law non-Newtonian fluid in the thermal developing region in an annulus. The steady state, two-dimensional heat transfer model is formulated and simulated by using an implicit finite difference method to investigate the effects of several dimensionless parameters on the heat transfer characteristics. The present numerical solution for a special case is found to be in excellent agreement with the previous one obtained by a semi-analytic method. The accuracy of the finite difference method, means that numerical results of temperature profiles and the Nusselt numbers can be generated for a wide spectrum of physical parameters which will provide useful and relevant information for process equipment design.

REFERENCES

1. Z. Tadmor and C. G. Gogos, *Principles of Polymer Processings*. Wiley Interscience, New York (1979).
2. D. R. Heldman, *Food Process Engineering*, 2nd Edn. Avi Publishing Co., Westport, CT (1988).
3. K. N. Strafford, P. K. Datta and C. G. Googan (Editors), *Coatings and Surface Treatment for Corrosion and Wear Resistance*. Ellis Horwood, Chichester, U.K. (1984).
4. S. N. Hong and J. C. Mathews, Heat transfer to non-Newtonian fluids in laminar flow through concentric annuli, *Int. J. Heat Mass Transfer* **12**, 1699–1705 (1969).
5. S. H. Lin, Heat transfer to plane non-Newtonian Couette flow, *Int. J. Heat Mass Transfer* **22**, 1117–1123 (1979).
6. S. H. Lin and D. M. Hsieh, Heat transfer to generalized Couette flow on non-Newtonian fluid in annuli with moving inner cylinder, *J. Heat Transfer, Trans. ASME* **102**, 786–790 (1980).
7. B. Carnahan, H. A. Luther and J. O. Wilkes, *Applied Numerical Methods*. Wiley, New York (1969).

TRANSFERT THERMIQUE POUR UN ECOULEMENT DE COUETTE DE FLUIDE NON NEWTONIEN DANS UN ESPACE ANNULAIRE AVEC CYLINDRE EXTERNE TOURNANT

Résumé—On étudie le transfert thermique d'un écoulement généralisé de Couette pour un fluide non newtonien à loi puissance dans un espace annulaire avec cylindre externe mobile. Les équations, sous forme intégrale, de la distribution de vitesse sont développées pour l'écoulement généralisé dans lequel la vitesse maximale peut apparaître entre les deux cylindres où sur le cylindre externe, suivant le gradient de pression imposé. Le modèle de transfert de chaleur qui inclut la dissipation visqueuse est traité numériquement pour les conditions aux limites de température constante. Les solutions numériques s'accordent bien avec celles semi-empiriques connues dans un cas particulier. On explore les effets des paramètres adimensionnels tels que le gradient de pression inverse, l'indice pseudoplastique et le paramètre de dissipation visqueuse, sur les caractéristiques du transfert thermique.

WÄRMEÜBERGANG IN EINER VERALLGEMEINERTEN NICHT-NEWTONSCHEN COUETTE-STRÖMUNG IN EINEM RINGSPALT MIT BEWEGTEM ÄUSSEREN ZYLINDER

Zusammenfassung—Es wird der Wärmeübergang in einer verallgemeinerten Couette-Strömung eines nicht-Newtonschen ('power-law') Fluids in einem konzentrischen Ringspalt mit bewegtem äußerem Zylinder untersucht. Die Gleichungen für die Geschwindigkeitsverteilung in der verallgemeinerten Strömung werden in Integralform entwickelt, wobei die Maximalgeschwindigkeit zwischen den beiden Zylindern oder am bewegten äußeren Zylinder auftreten kann. Dies hängt vom aufgeprägten Druckgradienten ab. Das Wärmeübergangsmodell enthält die viskose Dissipation und wird für die Randbedingung konstanter Zylindertemperatur numerisch gelöst. Die vorgelegten numerischen Ergebnisse stimmen sehr gut mit früheren halbanalytischen Lösungen für einen Spezialfall überein. Der Einfluß einiger dimensionsloser Parameter wie der Kehrwert des Druckgradienten, der Plaseudoplastik-Index und der Parameter für die viskose Dissipation auf die Charakteristik des Wärmeübergangs werden untersucht.

ТЕПЛОПЕРЕНОС К ОБОБЩЕННОМУ ТЕЧЕНИЮ КУЭТТА НЕНЬЮТОНОВСКОЙ ЖИДКОСТИ В КОЛЬЦЕВЫХ КАНАЛАХ С ДВИЖУЩИМСЯ ВНЕШНИМ ЦИЛИНДРОМ

Аннотация—Исследуется теплоперенос к обобщенному течению Куэтта степенной неньютоновской жидкости в концентрических кольцевых каналах с движущимся внешним цилиндром. Получены уравнения распределения скоростей в интегральной форме для обобщенного течения, скорость которого максимальна между обеими цилиндрами или у движущегося внешнего в зависимости от налагаемого градиента давления. Численно решается модель теплопереноса, включающая вязкую диссипацию, при граничных условиях с постоянной температурой цилиндра. Численные решения хорошо согласуются с полуэмпирическими, полученными ранее для определенного случая. Исследуется влияние, оказываемое на характеристики теплопереноса такими безразмерными параметрами как обратная величина градиента двления, показаталь псевдопластичности и параметр вязкой диссипации.